

## Investigation of Geothermal Sites in Korea\*

So Gu Kim\*\*

**Abstract:** Geothermal heat flow distribution of Korea is investigated in the light of geophysical data, seismicity, tectonics and gravity as well as heat flow measurements and surface temperature of hot springs. The average heat flow in Korea is found to be  $1.65\mu\text{cal}/\text{cm}^2\cdot\text{sec}$  that is greater than the world's average ( $1.5\mu\text{cal}/\text{cm}^2\cdot\text{sec}$ ). The high heat flow is located at the regions of high seismicity in Korea. They are found to be Bugok of south central, and Haeundae, Pohang and Dongnae of the southeast coast in the Peninsula. The anomalously high heat flow, equal to or greater than  $1.93\mu\text{cal}/\text{cm}^2\cdot\text{sec}$  is found in the Kyongsang Basin, indicating that it is extended from the spreading of the East Sea (Japan Sea) and its origin.

### INTRODUCTION

Nowadays many countries (e.g. Italy, N.Z., Japan, U.S.A., U.S.S.R. etc) are emphasizing on exploring for new geothermal areas and developing new ways to extract work from steam and hot water. The sources of usable geothermal energy in the earth fall into three classes: dry steam fields, wet steam fields, and the low temperature fields below the boiling point (at atmospheric pressure). The dry steam fields are filled mainly with steam itself, under pressure and at relatively high temperature. This steam is usable directly for the production of electric power. The steam from a dry field can be used other than power production. The water condensed from the steam after it has given up its energy can provide a supply of fresh water. So far such dry steam fields are as follows: the Larderello field in Italy, the Geysers field in California, the Volle Caldera field in New Mexico, and two fields in Japan.

The wet steam field is filled with hot water ( $>100^\circ\text{C}$ ) that does not become steam until

\* This study is supported by Department of Education, based on Academic Research Development. The author acknowledges its grant.

\*\* Dept. of Earth & Marine Sciences Hanyang University

the pressure is released by drilling into the field. The super-heated water in the wetfield at temperatures from  $180^\circ\text{C}$  to  $370^\circ\text{C}$  flashes into mixture of steam and water as it comes to the surface. Wairakei of N.Z., El Tatio of Chile, same fields of Iceland, Japan, and Chile are examples of the wet steam fields.

Finally the third type of a low-temperature field has only recently begun to receive attention. The low-temperature field generally consists of large bodies of water in the range of  $50^\circ$  to  $82^\circ\text{C}$ . The hot water from this field is most efficiently used for heating: in houses, greenhouses, mines in cold climate and industrial plants.

It is well-known that the Pacific Plate subducts under the Eurasian Plate at the Japanese arc and the frictional and conductive heating of the plate in the subduction zone give rise to a partial melting at the lower crust and the upper mantle of the East Sea. Furthermore the seismological investigations indicate that there were active volcanoes near Mt. Paektu (1597, 1668, 1702, and 1724) and Mt. Halla (1002, 1007), respectively (Kim, 1980). The hot spots of isolated volcanic regions, therefore, can not be ruled out in the Korean Peninsula.

Nevertheless papers on geothermal energy in

Korea are hardly found so far (Chang, 1920, Mizutani et al, 1920; and Kim, 1984). The objective of this paper is to provide the more precise geothermal sites and state of the art based on previous studies.

## BASIC THEORY OF HEAT FLOW

Heat transfer can take place essentially through three processes of conduction, convection and electromagnetic radiation. In heat flow measurements one usually takes into account conduction in which the transfer occurs through solid and convection in which a fluid moves a closed circuit and carries heat. It is found that there is a striking feature in the equality of the average heat flux for continents and oceans. Much of the heat flux at the surface of continents can be accounted for by the total heat production within the continental crust by radioactive decay. By contrast, radioactive decay in the oceanic crust can account for only a few percent of the oceanic heat flux.

Continental and oceanic heat flow measurements have been discussed by many geophysicists (e.g., Lachenbruch, 1970; Turcotte and Oxburgh, 1972; Schubert and Anderson, 1974). Surface heat flux  $q$  is linearly related to the heat production  $S(0)$  of radioactivity in surface plutonic rocks,

$$q = q^* + DS(0) \quad (1)$$

where  $D$  is a measure of depth over which the upper crustal radioactive heat sources are important,  $q^*$  is a measure of the heat flux into the crust from the underlying mantle and  $S(0)$  is heat production function. Should the heat production equation be the exponential function, the heat production of radioactive heat sources in the crust decreases with depth  $Z$

$$S(z) = S(0)e^{-z/D} \quad 0 \leq z \leq Z^* \quad (2)$$

The geotherms whose curves represent the variation of the earth's temperature with depth

are given with the exponential function of heat production.

$$T(z) = \frac{1}{K} [q^*z + D^2S(0)(1 - e^{-z/D})] \quad (3)$$

where  $K$  is the thermal conductivity

In an oceanic province, the cooling of the thermal boundary layer is governed by the simple differential equation in case of assumption of no major heat source.

$$\frac{\partial T}{\partial t} = k \frac{\partial^2 T}{\partial z^2} \quad (4)$$

where  $T$  is the temperature,  $Z$  is the depth and  $k$  is the thermal diffusivity. At  $Z=0$  the temperature must equal  $T_0$ , the temperature of the ocean floor, and as  $Z \rightarrow \infty$ ,  $T \rightarrow T_m$  the isothermal core temperature of the convective cell.  $T = T_m$  at time  $t=0$ , that is along the axis of the spreading ridge, the solution of equation(4) is

$$q(z) = (T_m - T_0) \operatorname{erf} \left( \frac{z}{2\sqrt{kt}} \right) \quad (5)$$

and surface heat flux  $q$

$$T_m - T_0 = \frac{\sqrt{\pi kt}}{K} q \quad (6)$$

where  $k$  is the thermal diffusivity and  $t$  is time.

## GEOHERMAL DATA AND ANALYSIS

Fig. 1 shows the tectonic linearments and faults in South Korea. Kim (1980) stated that the highest seismicity was found to be southeast of the Peninsula in the light of statistical analysis of instrumental and historical earthquakes (See Figure 2). In the Mesozoic rock of the Kyongsang Basin, ten large earthquakes whose intensities (MM Scale) are greater than 7 are observed along the Kyongsang Area where the Yangsan fault runs.

The high positive Bouguer anomalies are observed in Kyongsang Basin (See Figure 3). The high Bouguer gravity anomalies account for the crustal structures of high density which are complicately composed of sedimentary rock and

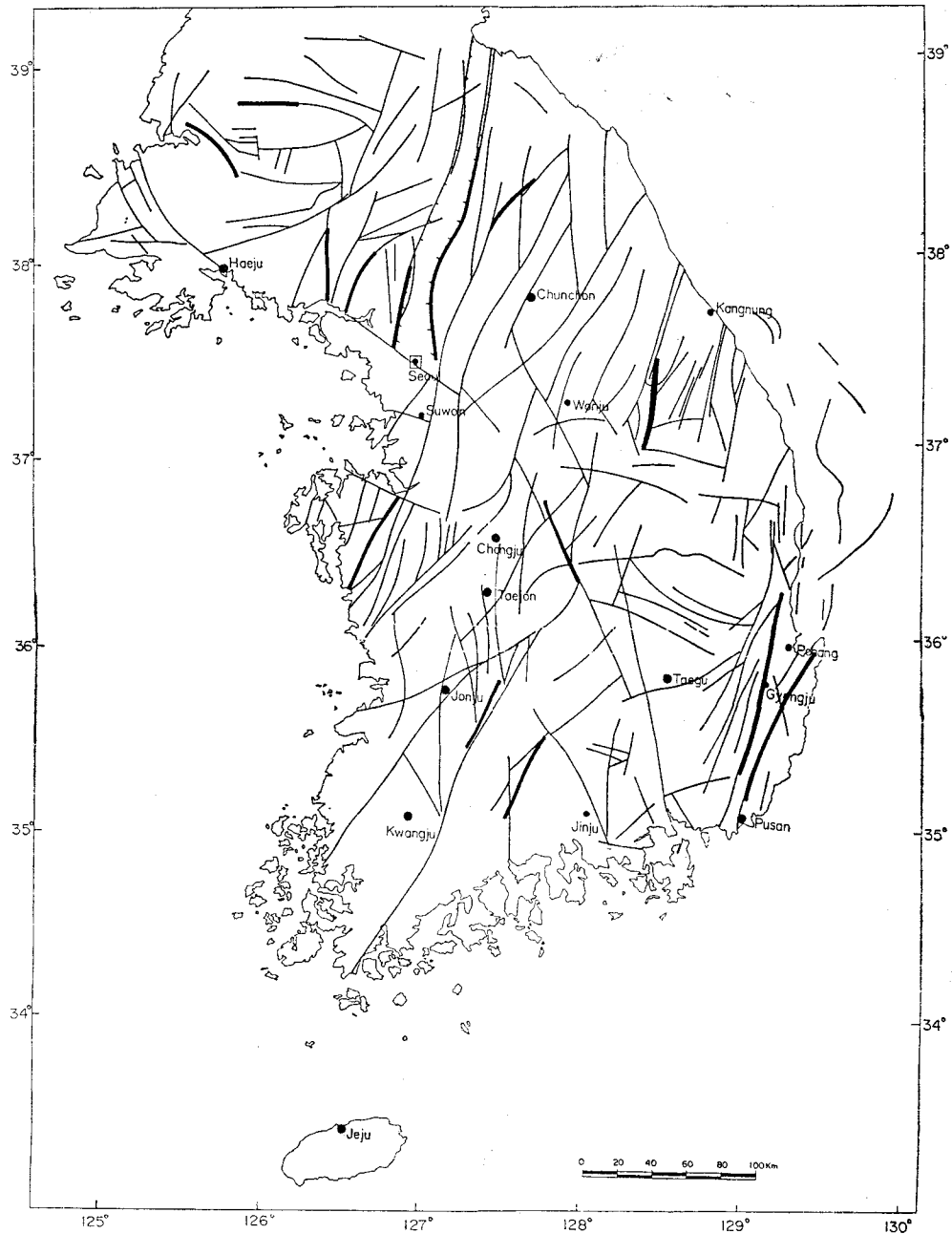


**Fig. 1** The tectonic lineaments and faults in Korea.

intrusive volcanic rock of ultramafic bodies. Such volcanic basin may also arise from the development of magma chambers in the lithosphere and the collapse of such chambers with concomitant accumulation of bedded volcanic

rocks on the surface. The map of geothermal springs (See Figure 4) and Table 1 show ten geothermal regions above 40°C in South Korea. Relatively high surface temperatures are observed at most of hot springs in the Kyongsang Basin

**Table 1** General description of thermal localities in Korea (Lim, 1983).

No	Name	Geology	Configuration	Temperature
1	Cheoksan*	Biotite granite (Bulgugsa)	N70E, 85NW	initial ejection 29°C present 42°C
2	Osaek	Biotite granite(Bulgugsa) Intrusion of porphyritic granite		28.9°C original well 32.9°C exploration well
3	Icheon	Biotite granite (Daebo)	Intrusion of felsite	Natural ejection 28~30°C temperature grad 40~70°C/Km
4	Onyang*	Porphyritic, hornblende, biotite granite (Daebo) Weathering depth; maximum 50m Intrusion of Pegmatite		first ejection 43~50°C present 50~58°C temperature grad 80.4°C/km
5	Dogo	Biotite granite(Daebo)	N10—30E along the intrusion of quartz porphyry	28°C
6	Deoksan*	Biotite granite and hornblende granite (Daebo)	N10—35W	initial temperature 33°C present 44°C temperature grad 80~91°C/km
7	Yuseong*	Biotite granite (Bulgugsa) Intrusion of quartz porphyry	E-W fault (10km) 50×800m	first 40°C present 41.5~50.3°C
8	Unheungri	Biotite granite (Bulgugsa) Deep weathering depth	N5-10E	natural ejection 22°C at 400m depth 24°C temperature grad 30°C/km
9	Suanbo*	Ogcheongye Phyllite crystalline-limestone	N80E fault	initial ejection 43°C present 51°C temperature grad 100~119°C/km
10	Deokguri	Granite gneiss	Intersection of N60E and N30E directions	first 34.9°C~36.7°C exploration well 39.5°C
11	Baegam*	Biotite, hornblende granodiorite (Daebo)	N5E EW	natural ejection 38~44°C exploration well 46~53°C
12	Pohang	Tertiary porphyrite (Gyeongsang supergroup)	Underlying the Tertiary Strata NNE fault	initial ejection 42°C present 39°C temperature grad 52°C/km
13	Okmyung	Agglomerate (Tertiary)	N80W	natural ejection 23°C
14	Jayang	Sedimentary rocks (Tertiary)	Anticlinal axis: N70W	ejection temperature 23°C
15	Gyeongsan	Gyeongsang supergroup shale, hornfels	N60E fault Fault breccia, calcite	initial ejection temperature 21°C
16	Chungdo	Gyeongsang supergroup shale, sandstone		mineral spfing 17°C exploration well 26°C(170m depth)
17	Bugok*	Gyeongsang supergroup shale, chert	N80W fault, Fault breccia, calcite 500(120~50)m	exploration well 21°C present 73°C(Max)
18	Yeongsan	Gyeongsang supergroup shale, chert	N80W	initial ejection 23°C present 29°C(170m depth)
19	Mageumsan*	Granite granodiorite (Bulgugsa)	N55~70W Fault breccia, calcite	present 42°C temperature grad 80.4°C/km
20	Jeongri	Grantie (Bulgugsa)	N5E	21.5°C ejection temperature grad 10~12°C/km

21	Dongnae*	Biotite granite (Bulgugsa) granitic prophyry	N5~10E fault	67°C present 54~56°C
22	Haeundae*	Hornblende, biotite granite granitic porphyry (Bulgugsa)		present 42~61°C

\* &gt; 40°C

Table 2 Heat flow measurements in the Republic of Korea.

Station No.	Section Name	Type	Lat.	Long.	Mizutani <i>et al.</i> (1970)			Chang (1970)			Mean
					K	dT/dZ	q	K	dT/dZ	q	$\bar{q}$
1	Tongyang	talc	36 57'	128 00'	8.1	1.5	1.2	6.95	1.50	1.04	1.12
2	Chungju	iron	36 57'	127 57'	6.7	2.4	1.6	5.81	2.25	1.31	1.46
3	Bongmyong	graphite	36 43'	128 08'	9.7	1.6~2.1	1.5~2.0	9.45	2.40	2.27	2.01
4	Mulkum	iron	35 19'	128 59'	5.5	2.9	1.6	6.11	3.90	2.38	1.99
5	Kumpuk	copper	35 13'	128 22'	4.7	2.6	1.2	5.96	2.25	1.34	1.27
6	Koobong	gold	36 24'	126 46'	8.0	1.8	1.4	7.01	2.20	1.54	1.47
7	Suhsung	lead/zinc	36 35'	126 25'				4.96	2.50	1.24	1.24
8	Pochon	iron	38 03'	127 18'	5.6	2.6	1.4	6.75	2.25	1.52	1.46
9	Hongchon	iron	37 54'	128 00'	6.6	2.4	1.6	5.38	2.60	1.40	1.50
10	Yangyang	iron	38 05'	128 34'	4.8	2.75	1.3	7.30	2.50	1.83	1.57
11	Uljin	lead/zinc	37 06'	129 16'	6.1	1.8	1.1	7.82	1.90	1.49	1.30
12	Pohang	oil	36 01'	129 22'	4.7	5.2	2.45	4.76	4.90	2.33	2.39
13	Chongsong	copper	36 21'	129 06'				8.93	1.80	1.61	1.61
14	Sinyemi	zinc/lead	37 12'	128 40'				6.53	2.40	1.57	1.57
15	Yonwha	zinc/lead	37 04'	129 02'				6.67	2.50	1.67	1.67
16	Cholma	copper	35 18'	129 08'				7.11	3.00	2.13	2.13
17	Kuryong	copper	35 18'	128 38'				8.60	2.00	1.72	1.72
18	Yongyang	copper	36 38'	129 14'				6.60	3.40	2.24	2.24

K : thermal conductivity in  $10^{-3}$ cal/cm. sec. CdT/Zd : temperature gradient in  $10^{-2}$ °C/m $\bar{q}$  : heat flow in  $10^{-6}$ cal/cm. sec

of the Southeastern Region. Furthermore high heat flow is also observed in the Kyongsang Basin. From Table 2 and Figure 5, the average heat flow measurements are observed as  $1.65\mu$ cal/cm<sup>2</sup>. sec for South Korea and  $1.93\mu$ cal/cm<sup>2</sup>. sec for the Kyongsang Basin. These represent much greater values than world's average  $1.5\mu$ cal/cm<sup>2</sup>. sec. The high values of the Kyongsang Basin may explain some partial melting at the upper mantle.

The surprising linear relation between heat flow and heat production in plutons is easily explained in terms of an exponentially decrease of heat production with depth in the crust.

$D$ , decrement and  $q^*$ , heat flux into the crust from the underlying mantle are determined empirically from surface observations. Decrements,  $D$  and Heat flux,  $q^*$  are determined by computing slopes and intercepts of the linear relation by the Least Square method (See Figure 6).

By measurements of heat flow  $q$  and heat production  $S(0)$  with units  $10^{-3}$ cal/cm<sup>3</sup>.sec on exposed plutons (Lachenbruch, 1970),  $D$ , the depth to which the differences in heat production and,  $q^*$ , the contribution to the flux from deeper sources are easily determined in terms of the linear relation.

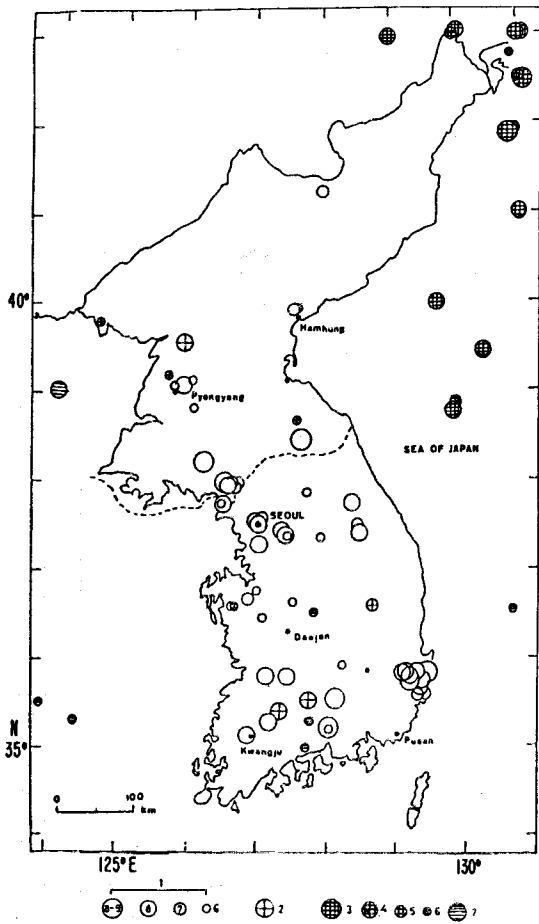


**Fig. 2** Epicenters of major earthquakes per year in Korea, compiled from historical earthquakes (27-1904 A.D.) and the records of the seismograph stations (1905~1979). Historical earthquakes are scaled by intensities (MM)

- 1—historical earthquake whose effect was limited in a small area.
- 2—historical earthquake whose effect was extended over a considerable territory
- 3— $M \geq 7.0$  for a depth of 300~700km
- 4— $7.0 > M \geq 6.0$
- 5— $6.0 > M \geq 5.5$
- 6— $5.5 > M \geq 5.0$
- 7—shallow depth ( $h \leq 60$ km)

Practically it is very difficult to measure the heat production of each different rock with present data, so that the quantity of the heat production is assumed to be grouped into 6 and 7 values of Basin and range for South Korea and Kyongsang Basin, respectively. This envis-

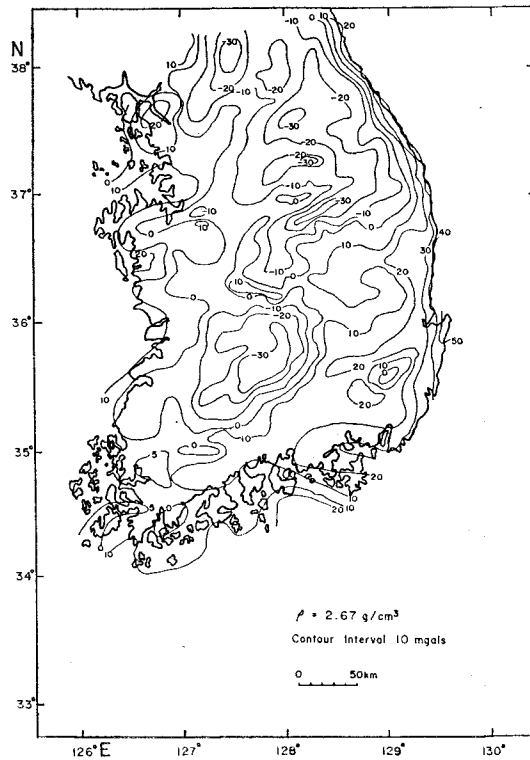


**Fig. 3** Bouguer gravity observations in the Republic of Korea.

aged model is drawn by assuming (1) that there is a steady-state heat flow and (2) that there exists a minimum depth  $Z^*$  across which the heat flow  $q(Z^*)$  is uniform throughout the province and (3) that the linear relationship between heat flow and heat production remain valid after differential erosion.

The heat flow parameters ( $q^*$ ,  $D$ ) are determined by means of the surface heat flow and heat production. The heat production, however, is not measured *in situ* here. It is postulated that the heat production is divided into a series of model values of normal high heat production for basin and range. Should the heat flow measurements for South Korea and Kyongsang Basin be grouped into the number of corresponding heat production respectively, the linear relationship between heat flow and heat production can be obtained as Figure 6. From Figure 6,

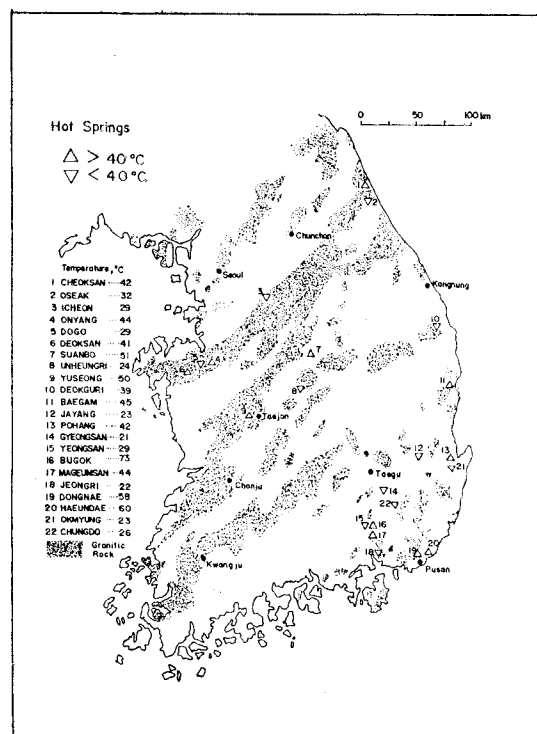


Fig. 4 The hot spring localities in the Republic of Korea.

the heat flow of the Kyongsang Basin is higher than that of South Korea. The larger value of  $q^*$  for the Kyongsang Basin is attributed to the heat flow through the upper mantle with the magma convection.

All observed geothermal activity in Korea is of the low temperature field. The maximum surface temperature amounting to 70°C and 60°C is observed at Bugok and Haeundae areas in the Southeastern region of Korea (See Table 1). It would appear to be a region of primary interest with regard to geothermal resources. Bugok currently develops 60°C~78°C waters with indicated reservoir temperatures of perhaps 120°~130°C. The spring occurs in N60°~80°W trending valley at or very near the intersection with a major N10°~20°W trending structure probably the Mageumsan springs. (Banks, 1980)

The temperature at 1150m in the petroleum exploration well of Pohang was reported as 99°C

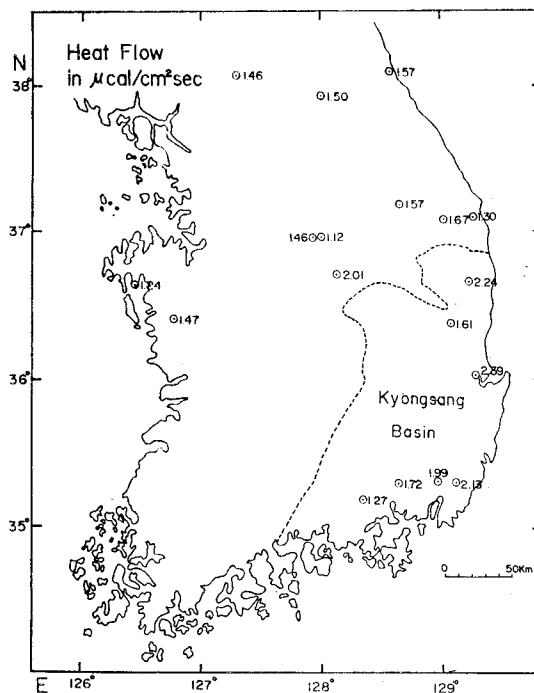


Fig. 5 Heat flow measurements in the Republic of Korea.

and the gradient on the temperature profile was recorded as relatively gradual even at the bottom of the hole. These observations suggest that the thermal water at Pohang might be different in nature from other thermal water localities. It is known that the Pohang thermal area is middle Tertiary tuffaceous sedimentary rock and the only one of Quaternary fault. The thermal water at Pohang takes place within a zone of NNE-Oriented faults.

## DISCUSSION AND CONCLUSION

The temperature profile beneath any pluton in a province is determined for any heat-flow province determined by ( $q^*$ ,  $D$ ). So if is probable to draw a family of temperature profiles for various values of the heat production  $S(0)$  on exposed plutons by using equation (3) and by assuming uniform thermal conductivity  $K=$

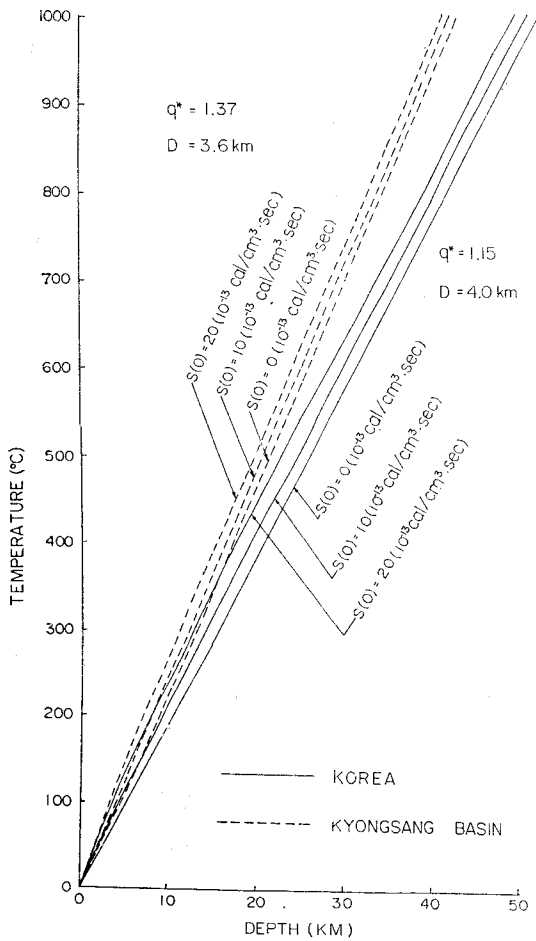


Fig. 6 Linear relation between heat flow and heat production in plutons of Korea.

6m cal/cm·sec°C. As shown on Figure 7, one can find that the shallower the depth is, the more heat production one observes, that is the heat production decreases exponentially with depth.

Figure 7 shows geotherms that represent the variation of the earth's temperature with respect to depth. As might be expected, the temperature found at a given depth in a region of high heat flow well be higher than the temperature at the same depth in a region of low heat flow. The gradient of the geotherms of the Kyongsang Basin is much steeper than those of South Korea, indicating that high heat flow is

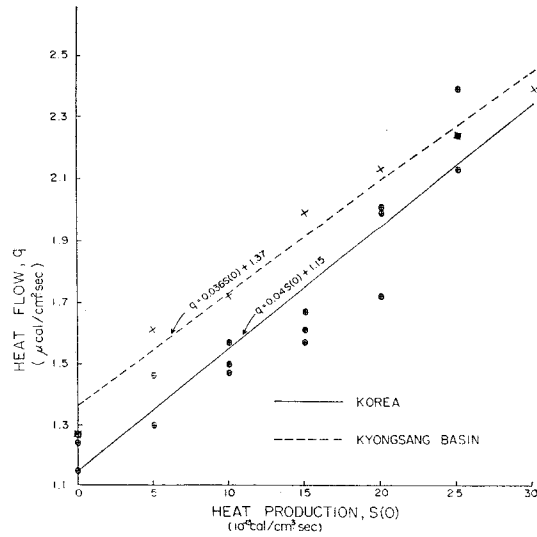


Fig. 7 Family of geotherms (curves representing the variation of the earth temperature with respect to depth) in Korea.

observed in the Kyongsang region. Kim(1983) estimated the crustal thickness of South Korea as 32km by using seismic wave in the Korean Peninsula. The depth of the base of the rigid lithosphere that is the onset of the partial melting is the onset of the partial melting is found to be deeply located below 55km in South Korea. This depth is called the low velocity zone seismologically. The partial melting below the crust of the Kyongsang Basin is due to the subducting movement of the Pacific Plate under the Eurasian Plate.

Bugok areas offer an excellent area for the development of the techniques that could be used for the enhancement and exploitation of the existing thermal water areas.

Pohang areas are also considered as geothermal sites for the low temperature field even if further investigation is needed in the future. Finally assessment of geothermal resources on the Island of Cheju is taken into account as the potential site based on its volcanic origin. The present geophysical data of Cheju, however, have been found insufficient geothermal utiliza-



tion. In order to investigate the above three regions, the detailed studies should be carried out by additional drilling, heat flow measurement in site, and Ocean bottom probe.

### REFERENCES

- Banks, N.C. (1980) Assesment of geothermal resources in the Republic of Korea, DOE.
- Bodvarsson, G. (1970) Evaluation of geothermal prospects and the objectives on geothermal exploration. *geoexploration*, 8, p.7-17.
- Chang, C.J. (1970) Heat flow in Korea. *Jour. Korean Inst., Mining Geol*, v. 10, p.23-46.
- Kim, S.G. (1980) Earthquake of the Korean Peninsula and its vicinity (Seismic risk of the Korean Peninsula and plate tectonics). *IISSE*, v. 18, p.101-126.
- Kim, S.G. (1984) Origin of the East Sea(Japan Sea) and plate tectonics. *the Jour. Oceano, soc. of Korea*, 19, p.94-102.
- Kim, S.J. and Kim, S.G. (1983) A study on the crustal structure of South Korea by using seismic waves. *Jour. Korean. Inst. Mining Geol*, V. 13, No. 1, p.1-19.
- Lachenbruch, A.H. (1970) Crustal temperature and heat production: Implication of the linear heat-flow relation. *Jour. Geophys. Res.* v. 75, p.3291-3300.
- Lim, J.W. (1983) Studies of characteristics and development on the Korean geothermals and hot springs, in *Research and Applied Geology of Korea*. KIER, 82-2-22, p.155-210.
- Mizutani, H., Boba, K., Kobayashi, N.K., Chang, C.C., Lee, C.H., and Kang, J.S. (1970) Heat flow in Korea. *Tectonophysics*, 10, p.183-203.
- Schubert, G. and Anderson, O.L. (1974) The earth's thermal gradient. *Physics Today*, p.28-34.
- Turcotte, D.L. and Oxburgh, E.R. (1972) Mantle Convection and the new global tectonics. *Annual Rev. of Fluid, Mech.*, 4, p.33-53.

### 한국의 지열부지에 관한 연구\*

金 昭 九\*\*

요약 : 지구물리학적자료, 즉 지열측정, 온천수의 온도는 물론 지진활동, 판구조력 및 중력등에 비추어 남한의 지열부지를 조사한다. 남한의 평균지열은 세계의 평균지열량( $1.5\mu\text{cal}/\text{cm}^2\cdot\text{sec}$ )보다 높은  $1.65\mu\text{cal}/\text{cm}^2\cdot\text{sec}$ 이다. 또한 높은 지열지대는 지진활동이 심한 지역과 일치한다. 이 높은 지열지대는 한반도의 동남부(경상분지)에 위치한 부곡, 해운대, 동래 및 포항등이다. 이 경상분지의 높은 지열이상은 평균  $1.93\mu\text{cal}/\text{cm}^2$ 이다. 이것은 동해의 높은 해저지열과 함께 동해의 확장 및 기원과 상호관계가 있음을 보여주고 있다.

\* 본연구는 문교부 학술연구 조성비의 지원을 받았다.

\*\* 한양대학교 지구해양학과